Electrocatalytic Oxidation Performance of PbO_2 Composite Electrode Doped with MXenes

Xinyu Zhang, Jiajun Li, Ming Guo*, Kaijie Ni, Ronghui Wu and Zhiyan Hu
College of Chemistry and Materials Engineering, Zhejiang Agriculture & Forestey University, Hangzhou, Zhejiang 311300, China.
guoming@zafu.edu.cn*

(Received on 14th April 2022, accepted in revised form 23rd December 2022)

Summary: In this study, a two-dimensional transition metal carbon/nitride (MXenes) method was used to enhance the electrocatalytic oxidation behavior of PbO_2 electrode. A novel composite electrode was prepared by doping the modified MXenes into PbO_2 material. The electrochemical performance was tested by electrochemical workstation. The typical cationic red X-GRL was treated by electrochemical oxidation, and the electrochemical oxidation performance of the material electrode was investigated. The results demostrated that the dyes were removed by the oxygen evolution reaction at the electrodes doped with modified MXenes by passing current. The charge transfer resistance is 12.56. The electrodes have remained stable after 20 cycles of charging and discharging. And the removal rate of cationic red X-GRL was as high as 95.19% in 120 min. A high-efficiency composite electrode was developed in this study, which increased the electrode's performance as well as wastewater degradation efficiency, and lay the groundwork for future research into doping MXenes to improve the performance of other materials. Hence, electrode materials doped with two-dimensional structured MXenes were candidates for the removal of contaminants, especially in the field of electrochemical catalysis.

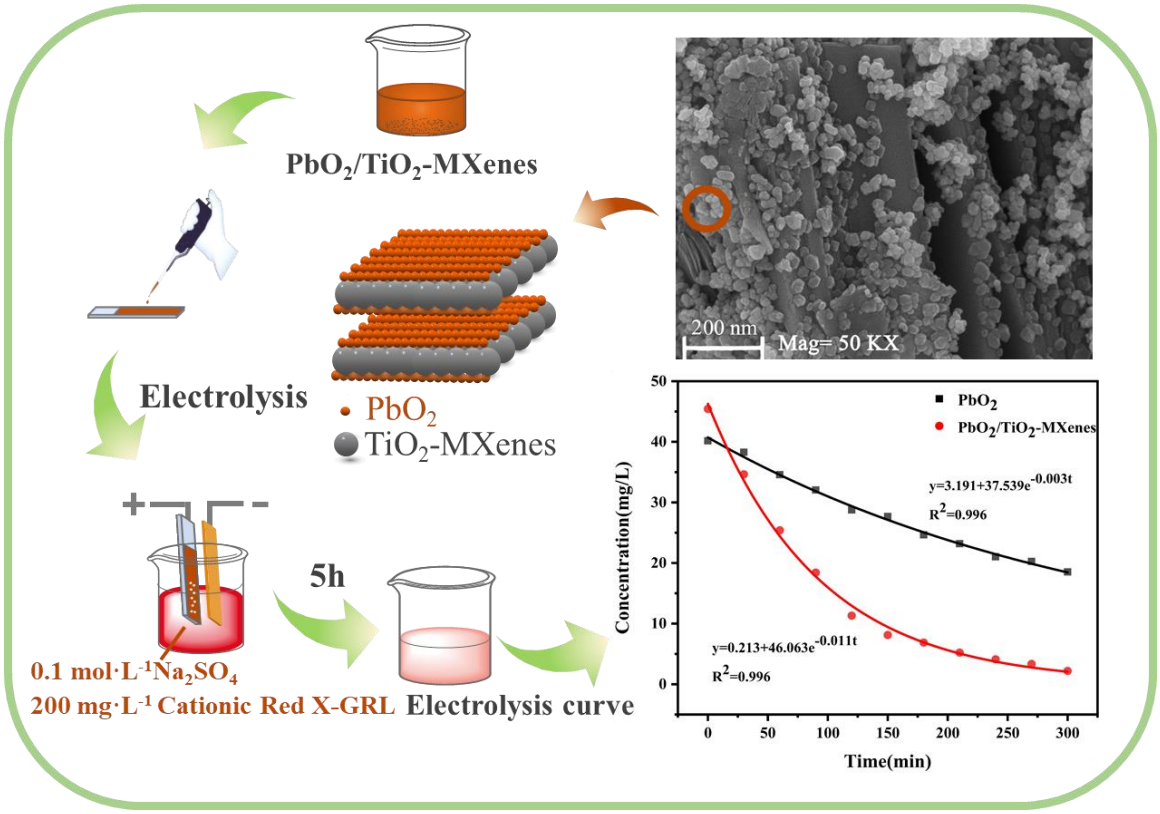

Key words: Two-dimensional transition metal carbon/nitride; PbO_2; Electrocatalytic Performance; Cationic red X-GRL.

*To whom all correspondence should be addressed.

Introduction

We have prepared PbO_2/HNT electrodes, a material with adsorption performance on wastewater, allowing charges to more effectively touch dye molecules and so improve the electrodes' waste reduction ability [1].

Advanced oxidation processes (AOPs) are commonly used to remove contaminants [2, 3]. The advanced oxidation process and electrochemical oxidation process function in combination, with proper pressurization, to produce various free radicals, such as hydroxyl radicals, which play a role in degradation and removal [4]. β-PbO_2 serves as an inactive electrode in the electrode material and undergoes little high oxidation with -OH radicals, thus requiring the compound of a more active anode [5]. Currently, graphene [6], TiO_2 [7], and SnO_2 [8] have excellent performance in electrochemical oxidation processes. Samarghandi [9] etc al. prepared a three-dimensional electrochemical reactor (3DER) with graphite, β-PbO_2 anode and activated carbon (GAC) particles by electrode precipitation method. The optimized 3DER was found to be much more efficient in catalytic degradation of BPA. The advantages of composite electrodes are the safety of the generated electrons as reagents, the tendency to automate the operation and the high efficiency [10]. However, the high cost remains a challenge that engineers keep trying to overcome. Hasani [11] *et al.* compounded SS316/β-PbO_2 electrode, which can enhance the efficiency of electro-Fenton process for degradation of hygromycin up to 100% under optimal conditions. The optimized anodic oxidation process can well improve the efficiency of the electrodes and reduce the cost [12, 13].

More recently, we found that doping with MXenes materials also enhance the behavior of electrodes and the effectiveness of wastewater treatment. MXenes, a novel type of two-dimensional material, has gotten a lot of attention because of its high potential for use in electrochemical energy storage. MXenes are two-dimensional layered materials made up of carbon/nitrogen/carbonitride transition metal complexes [14]. $M_{n+1}X_nT_X$ is the formula, where M is a premature metallic element, X is C or N, n = 1, 2, 3, and T_x is usually a surface terminal (mostly -OH, and -F). MXenes with chloride as the surface terminal were also reported [15]. MXenes flakes alone tend to decompose gradually in an environment containing oxygen and water, but show a reasonable stability in deoxygenated water or dry air [16].

Due to its advantages such as large layer spacing, excellent conductivity, good chemical stability, good hydrophilicity, and adjustable layer spacing, layered two-dimensional MXenes has great application and development prospects in the fields of batteries, supercapacitors and electrocatalysis [17, 18]. Or more 30 unique MXenes have been combined to date, with many more desired theoretically. [19, 20]. HF [21], NH_4HF_2 [22], LiF dissolved in HCl or LiCl dissolved in HF [23, 24] are among the most pervasive etchant agents that have been investigated yet. Other salts, such as NaF, KF, and CsF, can be used in place of LiF [23]. There is other – anti compounds, such as base chemicals [25, 26], and metal oxides fluorides, such as FeF_3 and CoF_2 [27-29]. Electrochemical etching [30] and molten salt etching [31] are two further etching processes. By soaking the Ti_3AlC_2-MAX phase in hydrofluoric acid solution, Yury's team [32] successfully synthesized Ti_3C_2-MXenes, the first member of the MXenes family. Professor Peng's [33] MXenes-Ag composite demonstrated good electrochemical activity in the REDOX reaction by boosting physical properties, increasing the number of active sites, and giving a synergistic effect. Bu [34] etc al. used carbide $Ti_3C_2T_x$-MXenes as composite material and polyvinyl alcohol (PVA) as substrate to form a $Ti_3C_2T_x$/MXenes-PVA composite with high dielectric constant by solution coating method. Cheng [35] etc al. prepared an emerging "Titanium-based" adsorbent, mp-MXene/TiO_2-x NDs, which was found to be highly efficient in the presence of H_2O_2 for the catalytic degradation of methyl orange dye by the Fenton reaction. However, the conditions involved are severe and require a specific light source as well as an additional catalyst. Othman [36] *et al.* prepared a composite AgNPs/TiO_2/$Ti_3C_2T_x$, loading both silver and palladium nanoparticles onto the composite surface, and demonstrated that the removal of MB from RhB was more than 85% within 120 min under the irradiation of simulated solar lamps. Similarly, the cost remains is a major challenge.

In this study, lead dioxide and MXenes modified by TiO_2 were used to prepare composite electrode materials with inexpensive preparation materials, a green and gentle process, simple operation, and easier progression towards automation, degrading cationic red dyes through an electrochemical oxidation process without the need for additional photocatalysis. The TiO_2/MXenes compound enables a larger proportion of Ti elements, which is more favorable for catalysis. Meanwhile, large cavities are formed between TiO_2 and C atoms on the surface of MXenes,

which facilitates the separation and transfer of charges, which plays a crucial role in the electrochemical oxidation process. The PbO_2/TiO_2-MXenes composite material was prepared by ultrasonically blending the TiO_2-MXenes and PbO_2 solution at high temperature, then subjected to heat preservation and pressure preservation. The performance of electrodes made from PbO_2/TiO_2-MXenes composite materials was investigated using galvanostatic, constant current charge-discharge technique, cross-circuit resistance method, and electrolysis technique. The entire experimental process is easy to operate and suitable for laboratory research.

Experimental

Materials

Experimental materials: ITO conductive glass, purchased from Shenzhen Nozor Co., Ltd., China. Lead oxide (PbO_2, >90% purity), purchased from Sinopharm Chemical Reagent Co., Ltd., China. MAX (Ti_3AlC_2, >90% purity), purchased from Jilin Technology Co., Ltd., China. Acetic acid (CH_3COOH, AR), sodium hypochlorite (NaClO, AR), anhydrous ethanol (CH_3CH_2OH, AR), hydrochloric acid (HCl, 36%), lithium fluoride (LiF, >80% purity), sodium sulfate (Na_2SO_4, >99% purity), alkaline Red 46 (cationic red X-GRL, AR), were purchased from Aladdin Co., Ltd., China. The water used in the experiments was all secondary distilled water.

Material Preparation

Preparation of PbO_2 by hydrothermal synthesis method: 2 g of lead oxide mixed in 20 mL of solution, drop in 1.1 mL acetic acid (AR), stir until the solution becomes clarified, and then regulate the pH to 9.0~10.0 with, add 80 mL sodium hypochlorite (AR), stir until the solution is brick red, react in an autoclave at 90 °C for 6 h, wait for the reactants to cool and dry, and wash with double-distilled water, anhydrous ethanol, respectively. Rinse and dry to obtain dark brown powder PbO_2.

Preparation of TiO_2-MXenes material: 1) The muffle liner was filled with a 20 mL HCl solution (note: glass reaction vessel cannot be used). After thoroughly stirring, 1 g LiF mixture was poured to the HCl solution, resulting in a homogenous mixed solution. The temperature was adjusted to 55 °C. 1 g of MAX (Ti_3AlC_2) powder was added slowly to the uniform mixed solution numerous times, and the temperature was maintained at a reasonable speed for 36 hours. The resulting mixture was diluted with a large amount of deionized water and washed by centrifugation. When the pH of the upper layer is about 6, the bottom sediment was separated and dried to obtain the sample MXenes-$Ti_3C_2T_x$ (T= OH, F or O).

2) The prepared powder sample was dispersed into deionized water. The same volume of pure reagent was added and evenly mixed, then transported to the reactor and maintained warm for 36 hours at 160 °C. The solution was placed and cleaned 2 - 3 times after the reaction was finished, then dried to yield TiO_2-MXenes powder.

Preparation of PbO_2/TiO_2-MXenes composite material: 50 mg of TiO_2-MXenes powder was dispersed to distilled water. The homogeneous dispersion was obtained by ultrasonication for 1 hour. An equal amount of PbO_2 was added to the homogeneous dispersion of TiO_2-MXenes. In 1 hour, an evenly distributed mixture was obtained, mixed and heated in an 80 °C water bath for 2 hours, and then placed in a 500 mL autoclave for 2 hours at 120°C. After the reaction solution cools down, draw and filter it, rinse it with double-distilled water, anhydrous ethanol and dry it respectively, and the precipitates obtained are PbO_2/TiO_2-MXenes composites.

Material Characterization

To study the morphology and elemental composition of PbO_2/TiO_2-MXenes electrodes, field emission scanning electron microscopy (SEM, Hithachi su8010, Japan), transmission electron microscopy (TEM, FEI Tecnai G2 F20, USA) were used for analysis. To determine the crystal structure of the electrodes, X-ray diffraction analysis (XRD, XRD 6000, Japan) was used for analysis. The phase analysis of the prepared PbO_2 samples was carried out using a powder X-ray diffractometer with Cu-Kα1 target (λ = 1.541 Å) as the radiation source at 2 θ = 10 ~ 80°, high voltage 40 kV and scan rate of 2 (°)/min. To study the electrochemical properties of the electrodes, an electrochemical workstation (CHI660C, China) was used for the analysis. To study the concentration of dyestuffs after degradation, UV-visible spectrophotometer (T6 New Century, China) and UV spectrophotometer analysis (UV-2550, Japan) were used. Plasma mass spectrometry (ICP-MS, XSERIES2, USA) was used for the elemental analysis of lead in the wastewater.

Preparation of electrodes and their performance testing

Preparation of electrodes: The prepared PbO_2/TiO_2-MXenes composite material was ultrasonically mixed with epoxy resin in the ratio of

4:1, and the dispersion was repeatedly applied dropwise on the surface of the conductive glass until the loading amount reached 5 $mg \cdot cm^{-2}$, at which time the PbO_2/TiO_2-MXenes/ITO electrode preparation was completed. PbO_2/TiO_2-MXenes electrodes anodes and stainless-steel mesh cathodes (equal area grids 1 mm × 1 mm) have the same dimensions (1 cm × 2 cm) and are placed parallel to each other inside the electrode at a distance of 2 cm.

The three-electrode system was established: PbO_2/TiO_2-MXenes/ITO electrode was used as the working electrode with a measurement area of 1 cm×2 cm, the auxiliary electrode is a platinum electrode, the reference electrode is a glyceryl electrode, and Na_2SO_4 is used as the electrolyte solution.

An electrochemical workstation was used to measure the EIS properties of PbO_2/TiO_2-MXenes composite electrodes (5 mV amplitude). The electrolyte solution used in the test was Na_2SO_4 (0.1 $mol \cdot L^{-1}$) and cationic red X-GRL (200 $mg \cdot L^{-1}$). The anode's galvanostatic test curves were recorded at different sweep speeds in the possible window of 0~2.0 V to see if redox peaks emerged. The anode's voltages charge and discharge test curve was captured at a 1 $A \cdot g^{-1}$ sweep rate, and the electrode under test was charged and discharged under constant current conditions to record its potential variation law over time in order to investigate the electrode's stability while charging and discharging.

Testing of electrolytic degradation of dyes

A DC power supply and electrodes formed the electrolytic device in the experiment. The cationic red X-GRL prepared in the laboratory was used as the contaminated wastewater and the results were indicated by UV-Vis spectrophotometer [1].

A PbO_2/TiO_2-MXenes/ITO electrode was chosen as the anode and a stainless-steel mesh of the same area was used as the cathode. The experiment was conducted at a current density of 2 $mA \cdot cm^{-2}$, pH = 9, temperature 25 °C, Na_2SO_4 solution concentration of 0.1 $mol \cdot L^{-1}$, volume of 200 $mg \cdot L^{-1}$ cationic red X-GRL solution 250 mL, stirring speed 200 $rpm \cdot min^{-1}$, constant current and slight change in voltage during experiment. During the electrolysis of the effluent, the samples were analyzed with a UV-Vis spectrophotometer to measure the absorbance values at 530 nm.

Standard curves were plotted: 2%, 4%, 6%, 8%, 10% (v/v) solutions of cationic red X-GRL were made. As a blank control, water was employed. The concentration of cationic red X-GRL was determined using the absorbance of the solution as measured by a UV-Vis spectrophotometer.

$$T_r = \frac{C_0 - C}{C_0} \quad (1)$$

where T_r is the removal rate, C_0 is the concentration of cationic red X-GRL water before treatment, and C is the concentration of treated water ($mg \cdot L^{-1}$).

Result and Discussion

Synthesis and Characterization of PbO_2/TiO_2-MXenes/ITO

X-ray diffraction (XRD) is widely used method to determine the crystalline phase of a material. As shown in Fig 1(a), in the spectra of MAX, MXenes and TiO_2-MXenes, in addition to the characteristic peaks of MAX, there are also peaks of (101), (200), (105), (211) in the TiO_2-MXenes spectra, 2θ corresponds to 25.30°, 48.04°, 53.88°, 55.06° of standard card TiO_2 (PDF No. 65-5714). It means that part of Ti on $Ti_3C_2T_x$ has turned into TiO_2. It is attributed to the accumulation of anatase TiO_2 particles in the titanium layer using MXene during hydrothermal oxidation [36]. According to the above information, the production of TiO_2 in TiO_2-MXenes material can be confirmed. From the comparison of the three samples, a very significant reduction peak at 38.47° can be observed. Through phase analysis, it can be found that this peak 2θ corresponds to 38.47° of standard card Al (PDF No. 65-5714), it can be inferred that the Al layer was successfully removed by etching. As shown in Fig. 1(b), the characteristic peaks of PbO_2 at 2θ = 25.40, 32.00, 36.23 and 49.10° are shown, which are assigned to the (110), (101), (200) and (211) planes respectively (PDF No. 41-1492). Meanwhile, the characteristic peaks of TiO_2 at 2θ = 48.04, 53.88 and 55.06°, which are assigned to the (200), (105) and (211) planes respectively (PDF No. 65-5714). It can be demonstrated again that TiO_2 has been formed in MXenes and successfully complexed with PbO_2.

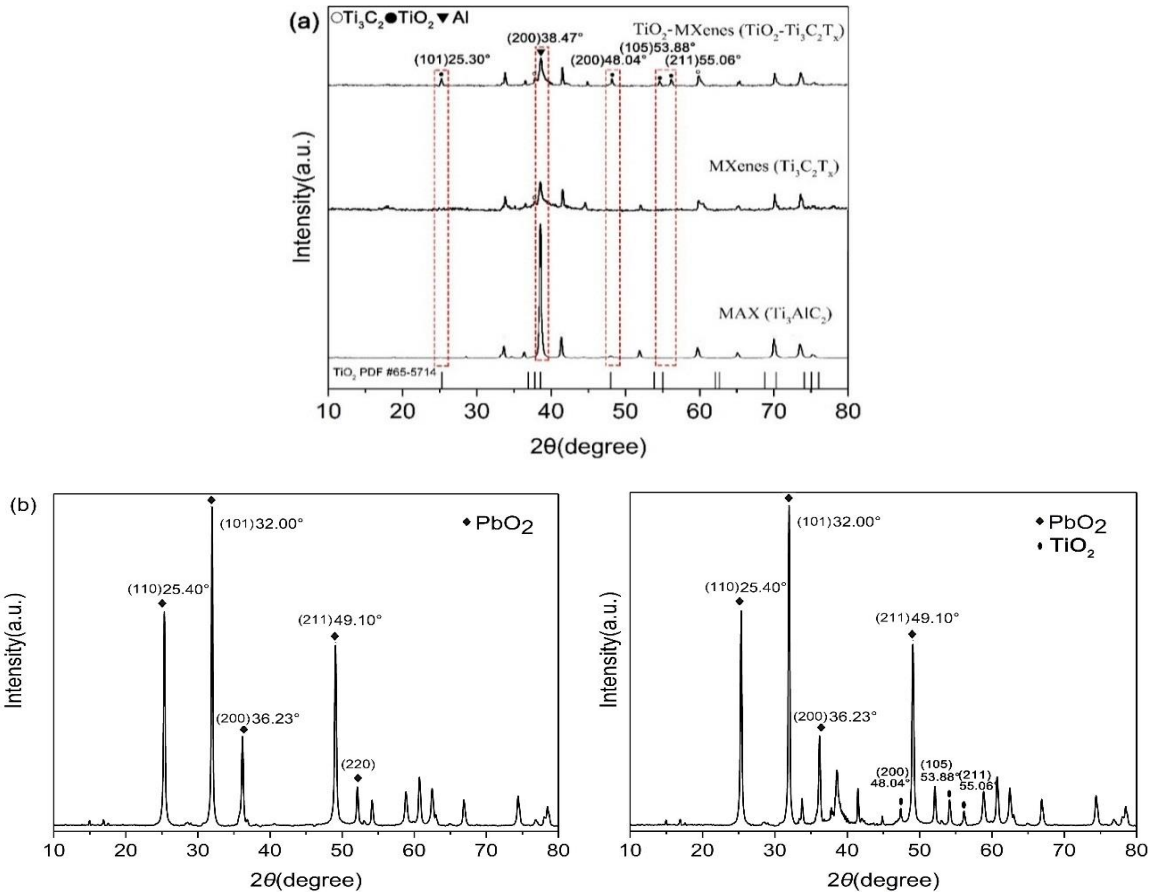

Fig. 1: XRD spectra of (a) MAX, MXenes and TiO_2-MXenes (b) XRD spectra of PbO_2/TiO_2-MXenes.

MAX, MXenes, TiO_2-MXenes, and PbO_2/TiO_2-MXenes composite materials are morphologically characterized, as shown in Fig 2(a) and (b), the MAX without the Al layer removed has no obvious layered structure, and the MXenes with the Al layer removed have the obvious layered structure; See the Fig 2(b) and (c), the surface of the MXenes material is relatively smooth (b), the surface of the TiO_2-MXenes material has an uneven particle structure (c), which is basically covered with the whole material. This significant difference indicates that the modification of MXenes was successful. Since the Al layer of MXenes material was removed, only Ti element in the material can be oxidized, therefore after modification, it is TiO_2-MXenes material. From the Fig 2(c) and (d), the particle size of PbO_2 is between 50-100 nm, and the gap of the TiO_2-MXenes layered structure is about 200 nm, so that the PbO_2 particles are embedded in it, and some particles are adsorbed in it. The surface of TiO_2-MXenes shows that PbO_2/TiO_2-MXenes materials are successfully composited. The PbO_2 particles embedded in TiO_2-MXenes enlarged the layer spacing of the original TiO_2-MXenes, allowing the electric charge to move more easily, which is the reason for the increased electrical conductivity of PbO_2/TiO_2-MXenes. Compared with the pure PbO_2 electrode, the conductivity of PbO_2/TiO_2-MXenes electrode and the contact area with dye wastewater are enhanced, while its degradability to dye wastewater is also improved. The scanning results by photoelectron spectrometer, as shown in Fig 3(a), suggest that the TiO_2-MXenes material mainly contains elements such as Ti, F, O and C, among which the content of Al is very small. It indicated that the Al layer has not been completely removed, but its content has reached a very low level; The high elements of F and O indicate that $Ti_3C_2T_x$ (T= OH, F or O) was successfully prepared for MXenes. To investigate the elements contained in the surface of the material, EDS analysis was performed. As shown in Fig 3(a), the material contains elements including Pb, Ti, O, F, and C. The TiO_2-MXenes material contains elements including Ti, O, F, and C. PbO_2 has the highest proportions, so the Pb element content is the highest. It can be judged by combining its SEM and EDS patterns in this experiment, PbO_2/TiO_2-MXenes composite material was successfully prepared.

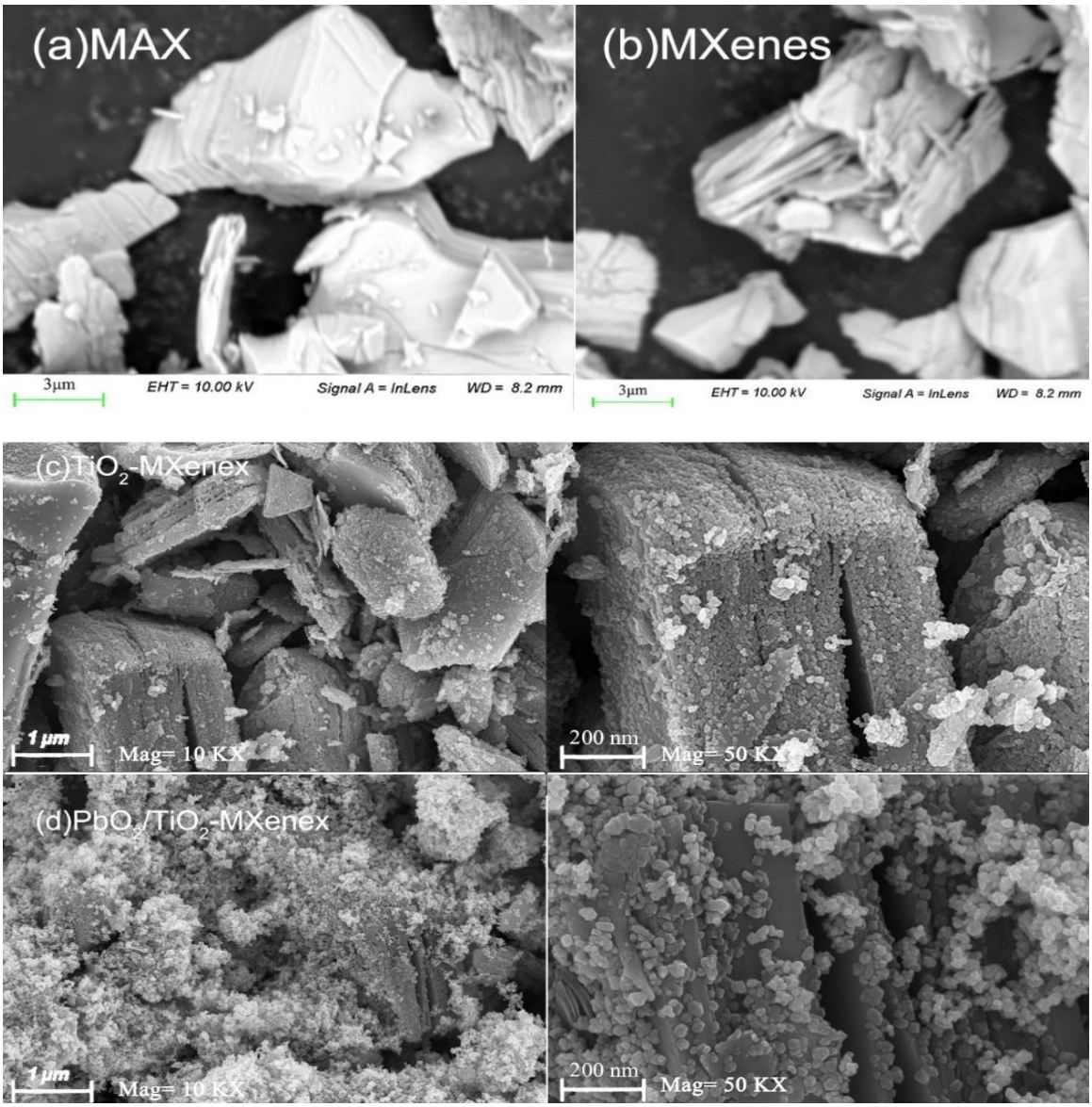

Fig. 2: SEM images of (a) MAX (b) MXenes (c) TiO_2-MXenes (d) PbO_2/TiO_2-MXenes.

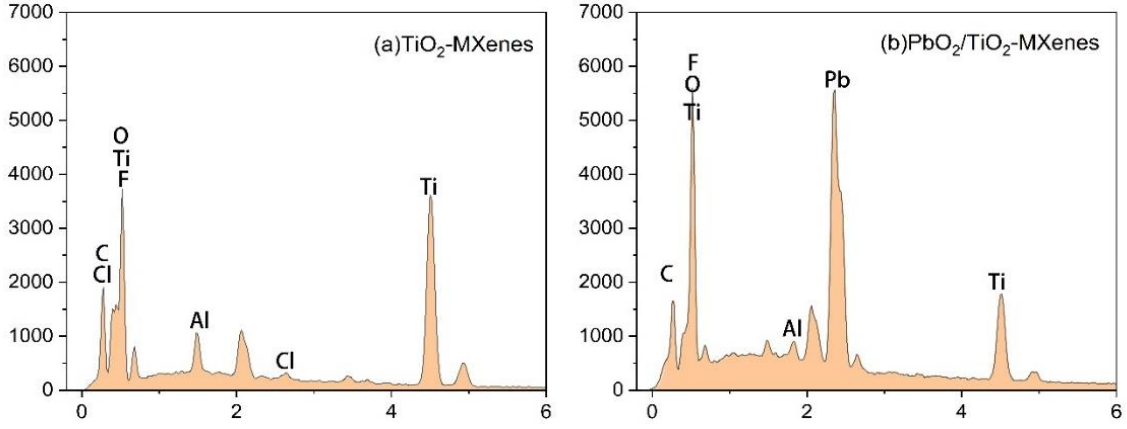

Fig. 3: EDS images of (a) TiO_2-MXenes and (b) PbO_2/TiO_2-MXenes.

Testing and Analysis of the Composite Electrode Performance

Loop Voltametric Curve Analysis

The ratio of the true surface area of the electrode to the specified surface area, which is known by relative surface roughness, one of the important parameters in electrocatalysis [37], is used to determine the values of the cyclic voltametric curve.

Fig. 4(a) shows the cyclic voltammogram of the electrode of PbO_2 material. The curves show regular symmetry in the scan range from 0 to 1.4 V, however, there is no rectangular feature, which can indicate that the electrochemical properties are inconspicuous. The cyclic voltammogram of the PbO_2/TiO_2-MXenes anode material is shown in Fig 4(b), which has good symmetry in the scanning range of 0 to 1.4 V and a more regular rectangular feature in the range of 0.3 to 1.1 V.

As can be seen in Fig 4(b), as the scanning speed increases, the response peak current of the electrode grows from 0.0025 to 0.007 A, the peak potential shifts from 1.38 to 1.22 V, and the area contained in the curve increases accordingly. When 0.1 mol·L^{-1} Na_2SO_4 and 200 mg·L^{-1} cationic red X-GRL were used as the electrolyte solution, no current flowed, the cyclic voltametric curves of the four electrodes did not scan the organic reduction peaks, and the electrodes could not directly electrochemically oxidize the cationic red X-GRL. After the application of current, a reduction peak appeared, and the reduction peak at 1.05 V first increased and then decreased with the increase of current, revealing that the cationic red X-GRL was gradually oxidized and degraded to produce the intermediate products. This was attributed to the fact that the lead dioxide electrode has a high oxygen evolution potential. In the electrolytic process, the anode generates strong oxidizing hydroxyl radicals to oxidize and degrade the dye [38]. Moreover, the curve is symmetrical, which implies a stable capacitive process for the composite electrode material [39].

Analysis of Galvanostatic Charge-discharge

Galvanostatic charge and discharge (GCD) is a frequently used method in electrochemistry to study the cell characteristics of electrodes and capacitors and to evaluate the cycle life of electrodes [40]. Fig 5(a) is the galvanostatic charge and discharge of PbO_2 material electrode. At a current density of 10 mA·g^{-1}, the charge and discharge curve of the PbO_2 composite electrode is symmetrical, showing that the electrode has high chemical traceability. It can be deduced from this statistic that it has a promising recycling life. The electrochemical electrical charges of the PbO_2/TiO_2-MXenes composite electrode is shown in Fig 5(b). The PbO_2/TiO_2-MXenes composite electrode exhibits substantially longer cycle charge and discharge periods than PbO_2 at a ratio of 10 mA·g^{-1}, and its charge and discharge curves are symmetrical. In the 500s cycle of charging, the PbO_2/TiO_2-MXenes electrode still runs stably after 20 cycles of charging and discharging, and the charging and discharging voltage remains stable. Therefore, the PbO_2/TiO_2-MXenes electrode has a good cycle life charging and discharging performance.

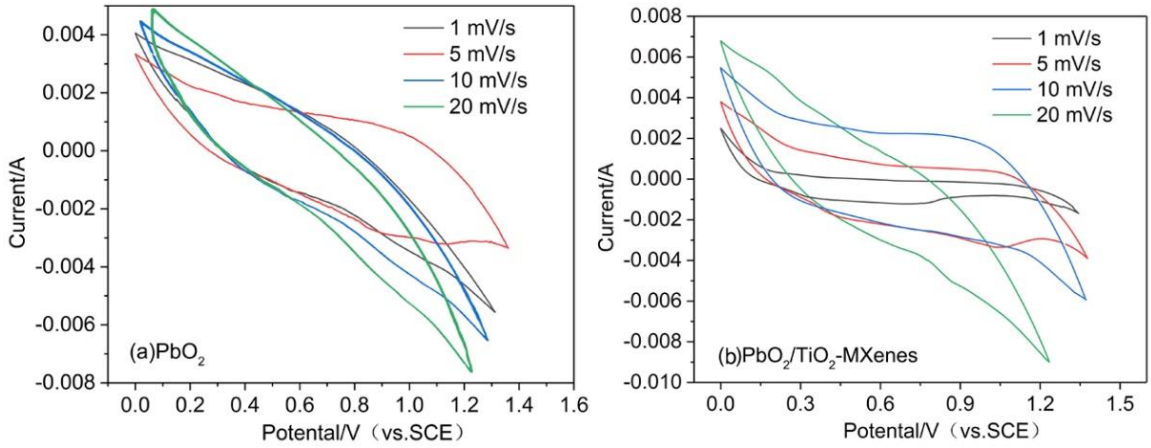

Fig. 4: Cyclic volt-ampf curves of nanometer (a) PbO_2 and (b) PbO_2/TiO_2-MXenes composites, scanning rate: 1 mV·s^{-1}, 5 mV·s^{-1}, 10 mV·s^{-1}, 20 mV·s^{-1}.

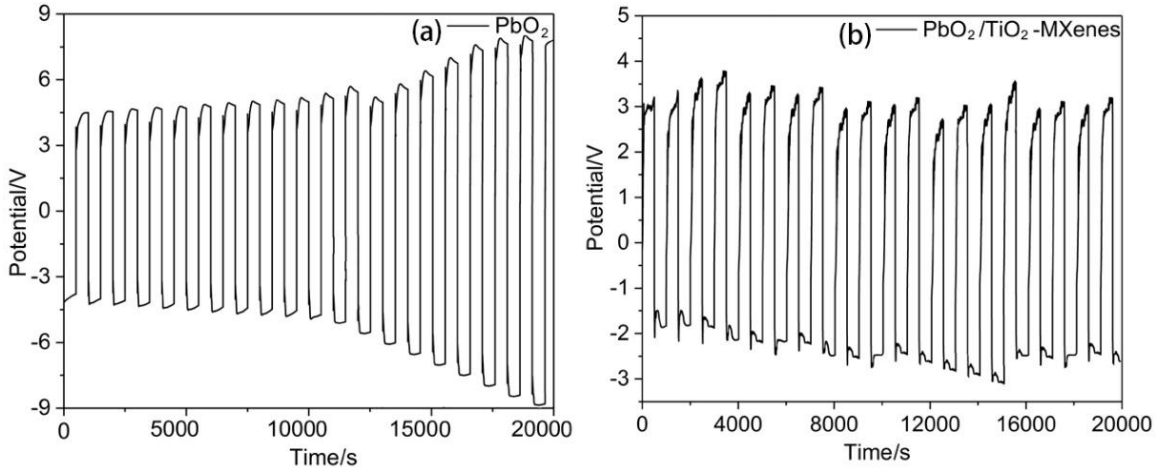

Fig. 5: Galvanostatic charge and discharge of (a) PbO_2 and (b) PbO_2/ TiO_2-MXenes electrodes, charge and discharge current: 10 $mA \cdot g^{-1}$.

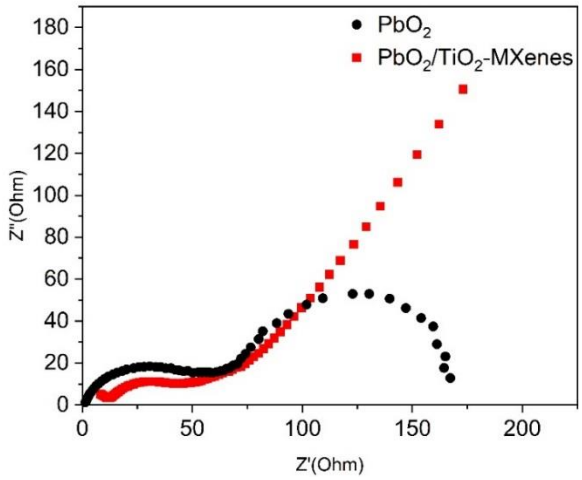

Fig. 6: PbO_2 and PbO_2/TiO_2-MXenes electrochemical impedance spectra.

AC Impedance Spectra of Electrodes

One of the most powerful instruments for studying the electrochemical process at the electrode/interface is Electrochemical impedance spectroscopy (EIS) [41]. In order to verify the electrochemical process of the electrode/interface, the PbO_2 electrode was compared with the PbO_2/TiO_2-MXenes composite electrode. According to the obtained electrochemical impedance spectroscopy (Fig 6), the equivalent circuit model (Fig 7) is determined, and the kinetic reaction, the mechanism reaction involved in the electrode system are estimated by establishing model. In our study an electrolyte of 0.1 $mol \cdot L^{-1}$ Na_2SO_4 was chosen for the EIS tests.

The impedance of the electrochemical system formed by the electrolyte and PbO_2/TiO_2-MXenes electrode mainly includes the impedance R_s of the electrolyte, the electric double layer capacitance C_{dl} generated by the charge between the interface, and the Faraday resistance impedance Z_f derived from the charge transfer and substance diffusion during the redox reaction. In addition, the existence of AC polarization makes Z_w occur in the capacitor. The general electrode reaction is usually composed of the charge transfer resistance R_1 of the electrode solution interface and the solution diffusion resistance. The Faraday resistance Z_f the system will change with the interface migration speed of the electrode reaction [42].

As shown in Fig 6 and Table 1, the PbO_2 electrode exhibited two large semicircle diameters, which were due to the oxidation its surface. After compounding the TiO_2-MXenes, their semicircle diameter was much smaller in diameter than those of the PbO_2 electrode and exhibited clear signs of diffusion resistance, indicating promoted charge transfer properties. The semicircle exhibited at higher frequencies is due to the charge transfer resistance R_1. The straight line at lower frequencies is due to Warburg impedance Z_w, which regulates the dispersal factor of sodium-ions. The solution diffusion resistance of PbO_2/TiO_2-MXenes composite electrode is much higher than the resistance of PbO_2, indicating that the composite electrode has a greater charge transfer resistance R_1 in solution and a smaller charge transfer resistance on the electrode, so the reaction speed on the electrode is faster, and the PbO_2/TiO_2-MXenes composite electrode has better conductivity.

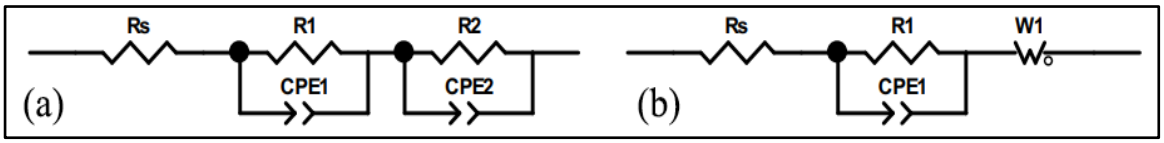

Fig. 7: (a) Equivalent circuit used for fitting of PbO_2 electrode (b) Equivalent circuit used for fitting of PbO_2/TiO_2-MXenes electrode.

Table-1: Electrode's solution resistance and charge transfer resistance.

Electrode name	R_s	R_1	CPE_1	R_2	CPE_2	W_1
PbO_2 electrode	0.814	57.840	0.751	119.4	0.836	-
PbO_2/TiO_2-MXenes electrode	1.753	12.560	0.921	-	-	0.177

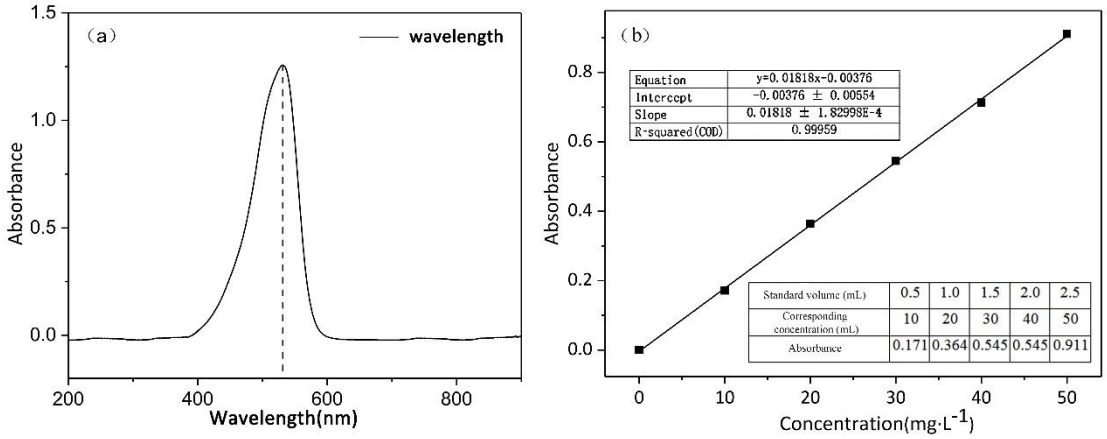

Fig. 8: (a) cationic red X-GRL absorption curve and (b) standard profile.

Determination of Standard Curve for Dye Wastewater

Preparation of Standard Curve

The results obtained from the UV spectrophotometer scan are shown in Fig 8(a). It can be seen that the wavelength of the absorption maximum is located at 530 nm. As a result, cationic red X-GRL absorbance must be measured at 530 nm [1].

The detected absorbance values were 0.171, 0.364, 0.545, 0.713, 0.911 by adding the standard solution in amounts of 0.5 mL, 1.0 mL, 1.5 mL, 2.0 mL, and 2.5 mL, respectively, based on the findings of measuring the absorbance of the standard solution by UV-Vis spectrophotometer. The concentration was represented as the bottom line, and absorbance was plotted as the vertical coordinate. The equation of regression was A=0.01818C-0.00376 and the correlation coefficient R^2=0.99966, where A is the absorbance and C is the concentration of the solution. cationic red X-GRL had good linearity in the range of 0-50 mg·L^{-1}, as shown in Fig 8(b).

Degradation kinetic curves of cationic red X-GRL by PbO_2/TiO_2-MXenes composite electrode

The degradation efficiency of PbO_2/TiO_2-MXenes composite electrode for cationic red X-GRL would be reflected by kinetic analysis. In our study, 250 mL of 200 mg·L^{-1} of cationic red X-GRL was taken and electro catalyzed for 300 min using an electrode with a loading of 5 mg·cm^{-2}. The supernatant was taken every 30 min and the absorbance of cationic red X-GRL was measured at the maximum absorption wavelength of 530 nm. When measuring the absorbance, the concentration was oversized, so the dye was diluted by a factor of 5. The degradation curves are shown in Fig 9. The kinetics of the catalytic degradation reaction at PbO_2/TiO_2-MXenes composite electrodes was calculated by the Langmuir-Hinshelwood (L-H) first-order kinetic model (Equation 2).

$$C = k_1 - k_2 e^{-k_3 t} \quad (2)$$

where C is the concentration change curve of cationic red X-GRL, t is the time, and k_1, k_2, and k_3 are the degradation rate constants.

Fig. 9(a) shows that the degradation rate is faster from 0 to 100 min, as the time continues, the removal rate gradually approaches the equilibrium and tends to the maximum removal rate. Calculated from the regression equation A=0.01818C-0.00376, the degradation rate of PbO_2/TiO_2-MXenes composite electrode was 95.19% in 5 hours. The probably factor is that the PbO_2/TiO_2-MXenes composite electrode rapidly generates a large number of hydroxyl radicals in contact with the solution on the surface after the current is applied, and the efficiency of generating reactive radicals decreases with time, leading to the slowdown of the removal efficiency. The relationship fitted to C-t, as shown in Fig 9(b), with $R^2 = 0.996$, indicates that the reaction compounds the first order kinetic law.

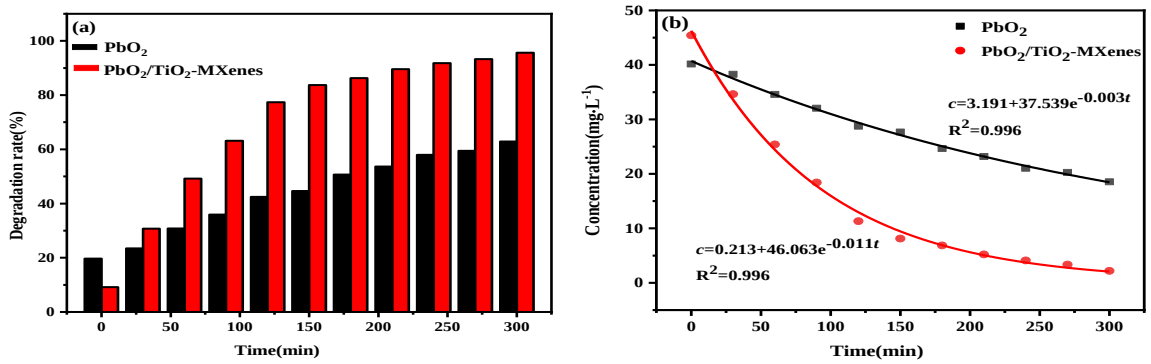

Fig. 9: (a) the degradation rate of PbO_2/TiO_2-MXenes composite electrode, (b) The first order kinetic curve of cationic red X-GRL, current density: 2 $mA \cdot cm^{-2}$, T = 25 °C.

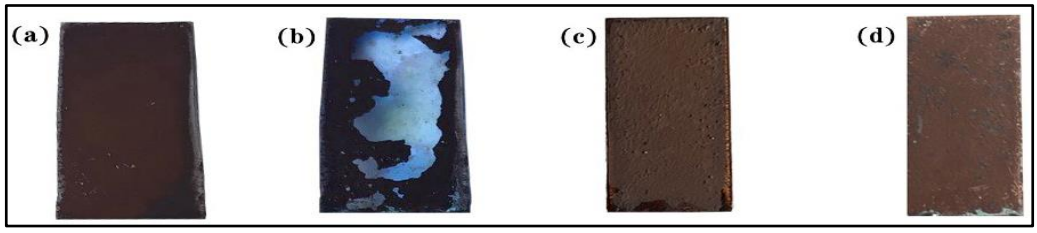

Fig. 10: (a) Before Electrolysis and (b) After Electrolysis are PbO_2 electrodes, (c) Before Electrolysis and (d) After Electrolysis PbO_2/TiO_2-MXenes electrodes.

As shown in Fig 10, through the comparison of the electrodes before and after working, it is found that the PbO_2/TiO_2-MXenes electrode hardly falls off. Because the TiO_2-MXenes material has unique conductivity and hydrophilicity, it has high chemical activity after etching and enhances the formation of functional groups such as hydroxyl groups. The PbO_2/TiO_2-MXenes material electrode exhibits good stability during the electrolysis process. It was observed that there was no obvious anodic oxidation on the electrode, explaining that the inclusion of TiO_2-MXenes boosted the adhesion and stability of the electrode. As shown in Table 2, the ICP-MS elemental chromatograms of the dye wastewater showed slight dissolution of both PbO_2 and PbO_2/TiO_2-MXenes electrodes. The solubility of the PbO_2/TiO_2-MXenes electrode was less than that of the PbO_2 electrode, indicating that the presence of MXenes enhances the reliability of the electrode, thus reducing the secondary contamination of water quality as a result of electrode solution. Table 3 shows that by comparing the dye degradation experiments reported in the literature [43-46], it was found that PbO_2/TiO_2-MXenes electrodes compounded with different materials showed excellent degradation efficiency under electrocatalytic conditions. In a similar work, our study appears to be less costly and simpler in operation, and the electrodes can be obtained by drop coating method during preparation without electrochemical deposition. Meanwhile, in terms of removal rate, our electrodes showed excellent degradation efficiency.

Table-2: ICP-MS Lead Element Analysis.

Electrode name	Electrolysis time (h)	Lead content ($\mu g \cdot L^{-1}$)
PbO_2 electrodes	0.000	0.000
PbO_2 electrodes	5.000	27.560
PbO_2/TiO_2-MXenes electrodes	0.000	0.000
PbO_2/TiO_2-MXenes electrodes	5.000	5.767

Table-3: Removal efficiency, operating conditions and cost comparison of pollutant degradation on different PbO_2 electrodes.

Sample	Removal efficiency (%)	Method	Catalyst conditions	Material preparation cost (RMB)	References
PbO_2/RGO	69.3%	Hydrothermal synthesis	Electrocatalyst	1784	[43]
Ti/Pt/TiO_2-PbO_2	95%	Anodic oxidation method	Electrocatalyst	2147	[44]
Ti/TiO_2-NTs/PbO_2	85%	Electrodeposition	Electrocatalyst	4034	[45]
Ti/TNTs/Fe-Ce-PbO_2	79.8%	Electrodeposition method	Electrocatalyst	3881	[46]
PbO_2/TiO_2-MXenes	95.19%	Hydrothermal synthesis method	Electrocatalyst	1184	This work

Analysis of the possible degradation mechanism of cationic red X-GRL

Free radicals generated by electrochemical oxidation processes are the main mechanism by which dyes can be degraded to smaller molecules, primarily in two ways: direct and indirect oxidation [39]. Under the action of electric current, the metal anode surface is exposed to water molecules and activated to hydroxyl radicals, oxygen radicals and other reactive radicals. These reactive radicals attack the cationic red X-GRL molecule, leading to the breakage of azo and amine bonds, etc., producing amines, benzoic acid, phenol, and other aromatic compounds. The continuous production of reactive groups within the system causes further decomposition of aromatic compounds into smaller molecules, formic acid, acetic acid, malonic acid, etc. These organic acids eventually degrade to CO_2, H_2O and simple inorganic ions [47].

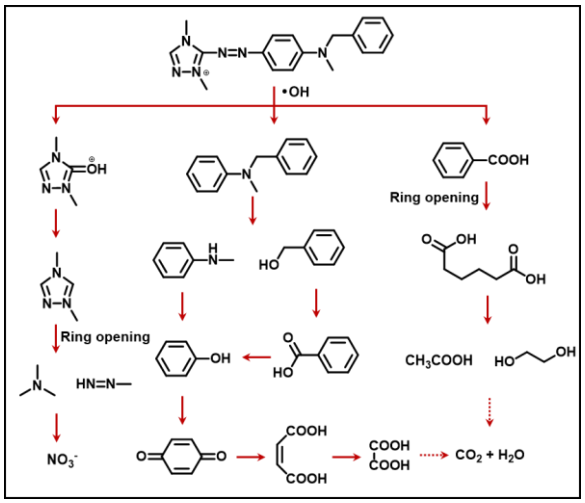

Fig. 11: Possible degradation process of cationic red X-GRL.

Conclusion

In our study, we prepared TiO_2-MXenes material by electrode drop coating method firstly by hydrothermal oxidation, and then compounded with PbO_2 to prepare PbO_2/TiO_2-MXenes electrode, and the success of the compounding was proved by characterization that the electrode is not easy to fall off. Compared with the single PbO_2 electrode, the composite electrode exhibited more excellent electrochemical performance with low charge transfer resistance, long lifetime, and high oxygen evolution potential, which could generate more and stronger reactive radicals for dye degradation. As evidenced from the removal rate, the PbO_2/TiO_2-MXenes electrode will reach the critical value after 3 hours of electrocatalysis, and the removal rate of cationic red X-GRL dye is high as 95.19%. However, it is still necessary to continue to explore the degradation conditions for cationic red X-GRL dye and the possibility of degradation for other pollutants in our study. Summarily, the composite electrode prepared in this work has high activity and stability, which provides a new way for water treatment field suitable for industrial production.

Acknowledgments

The Zhejiang public welfare Technology Application Research Project (LGN20B070001, LGN21B070001).

References

1. J. Li, M. Guo, Y. Shao, H. Yu and K. Ni, Electrocatalytic Properties of a Novel β-PbO_2/Halloysite Nanotube
2. Composite Electrode, *ACS Omega*., **6**, 5436 (2021).
3. A. Dargahi, H. R. Barzoki, M. Vosoughi and S. A. Mokhtari, Enhanced electrocatalytic degradation of 2,4-Dinitrophenol (2,4-DNP) in three-dimensional sono-electrochemical (3D/SEC) process equipped with Fe/SBA-15 nanocomposite particle electrodes: Degradation pathway and application for real wastewater, *Arabian J. Chem*., **15**, 103801 (2022).
4. A. Dargahi, M. Vosoughi, S. A. Mokhtari, Y. Vaziri and M. Alighadri, Electrochemical degradation of 2,4-Dinitrotoluene (DNT) from aqueous solutions using three-dimensional

electrocatalytic reactor (3DER): Degradation pathway, evaluation of toxicity and optimization using RSM-CCD, *Arabian J. Chem*., **15**, 103648 (2022).

5. A. Dargahi, K. Hasani, S. A. Mokhtari, M. Vosoughi, M. Moradi and Y. Vaziri, Highly effective degradation of 2,4-Dichlorophenoxyacetic acid herbicide in a three-dimensional sono-electro-Fenton (3D/SEF) system using powder activated carbon (PAC)/Fe_3O_4 as magnetic particle electrode. *J. Environ. Chem. Eng*., **9**, 105889 (2021).
6. M. R. Samarghandi, A. Dargahi, A. Rahmani, A. Shabanloo, A. Ansari and D. Nematollahi, Application of a fluidized three-dimensional electrochemical reactor with Ti/SnO_2–Sb/β-PbO_2 anode and granular activated carbon particles for degradation and mineralization of 2,4-dichlorophenol: Process optimization and degradation pathway. *Chemosphere*., **279**, 130640 (2021).
7. A. Dargahi, M. Moradi, R. Marafat, M. Vosoughi, S. A. Mokhtari, K. Hasani and S. Moghadami, Applications of advanced oxidation processes (electro-Fenton and sono-electro-Fenton) for degradation of diazinon insecticide from aqueous solutions: optimization and modeling using RSM-CCD, influencing factors, evaluation of toxicity, and degradation pathway, *Biomass Convers. Biorefin.* (2021). 10.1007/s13399-021-01753-x;
8. A. Dargahi, A. Ansari, D. Nematollahi, G. Asgari, R. Shokoohi and M. R. Samarghandi, Parameter optimization and degradation mechanism for electrocatalytic degradation of 2,4-diclorophenoxyacetic acid (2,4-D) herbicide by lead dioxide electrodes, *RSC Adv*., **9**, 5064 (2019).
9. A. Dargahi, D. Nematollahi, G. Asgari, R. Shokoohi, A. Ansari and M. R. Samarghandi, Electrodegradation of 2,4-dichlorophenoxyacetic acid herbicide from aqueous solution using three-dimensional electrode reactor with G/β-PbO_2 anode: Taguchi optimization and degradation mechanism determination, *RSC Adv*., **8**, 39256 (2018).
10. M. R. Samarghandi, A. Ansari, A. Dargahi, A. Shabanloo, D. Nematollahi, M. Khazaei, H. Z. Nasab and Y. Vaziri, Enhanced electrocatalytic degradation of bisphenol A by graphite/β-PbO_2 anode in a three-dimensional electrochemical reactor, *J. Environ. Chem. Eng*., **9**, 106072 (2021).
11. M. M. Mahmoudi, R. Khaghani, A. Dargahi and G. M. Tehrani, Electrochemical degradation of diazinon from aqueous media using graphite anode: Effect of parameters, mineralization, reaction kinetic, degradation pathway and optimization using central composite design, *Int. J. Environ. Anal. Chem*., **102**, 1709 (2022).
12. K. Hasani, S. Hosseini, H. Gholizadeh, A. Dargahi and M. Vosoughi, Enhancing the efficiency of electrochemical, Fenton, and electro-Fenton processes using SS316 and SS316/beta-PbO_2 anodes to remove oxytetracycline antibiotic from aquatic environments, *Biomass Convers. Biorefin.* (2021). 10.1007/s13399-021-01967-z
13. M. R. Samarghandi, A. Dargahi, A. Shabanloo, H. Z. Nasab, Y. Vaziri and A. Ansari, Electrochemical degradation of methylene blue dye using a graphite doped PbO_2 anode: Optimization of operational parameters, degradation pathway and improving the biodegradability of textile wastewater, *Arabian J. Chem*., **13**, 6847 (2020).
14. M. R. Samarghandi, D. Nemattollahi, G. Asgari, R. Shokoohi, A. Ansari and A. Dargahi, Electrochemical process for 2,4-D herbicide removal from aqueous solutions using stainless steel 316 and graphite Anodes: optimization using response surface methodology, *Sep. Sci. Technol*., **54**, 478 (2019).
15. M. Naguib, V. N. Mochalin, M. W. Barsoum and Y. Gogotsi, Two-Dimensional Materials: 25th Anniversary Article: MXenes: A New Family of Two-Dimensional Materials, *Adv. Mater*., **6**, 992 (2014).
16. E. Chang, M. Q. Zhao, M. Taron, H. Joseph, B. Muhammad, K. Sankalp, A. Babak, W. M. Michel and G. Yury, Porous Two-Dimensional Transition Metal Carbide (MXene) Flakes for High-Performance Li-Ion Storage, *Chemelectrochem*., **3**, 689 (2016).
17. O. Mashalir, K. M. Cook, V. N. Mochalin, M. Crowe, M. W. Barsoum and Y. Gogotsi, Dye adsorption and decomposition on two-dimensional titanium carbide in aqueous media, *J. Mater. Chem. A*., **2**, 14334 (2014).
18. M. R. Lukatskaya, R. Maria, Z. F. Lin, M. Q. Zhao, D. Mikhael, W. Michel, P. Simon and Y. Gogotsi, Ultra-high-rate pseudocapacitive energy storage in two-dimensional transition metal carbides, *Nature Energy*., **2**, 17105 (2017).
19. L. Andrew, K. Dilip and V. Venkatasubramanian, Exploring MXenes as Cathodes for Non-Aqueous Lithium–Oxygen Batteries: Design Rules for Selectively Nucleating Li_2O_2, *Chemsuschem.*, **11**, 1911 (2018).
20. B. Anasori, M.R. Lukatskaya and Y. Gogotsi, 2D metal carbides and nitrides (MXenes) for energy storage, *Nat. Rev. Mater*., **2,** 16098 (2017).
21. L. Verger, V. Natu, M. Carey and M. W. Barsoum, MXenes: An Introduction of Their Synthesis, Select properties and applications, *Trends Chem*.,

1, 656 (2019).
22. M. Naguib, M. W. Barsoum and Y. Gogotsi, Ten Years of Progress in the Synthesis and Development of MXenes, *Adv. Mater*., **33**, 2103393 (2021).
23. A. Sarycheva and Y. Gogotsi, Raman Spectroscopy Analysis of the Structure and Surface Chemistry of Ti_3C_2Tx MXene, *Adv. Mater*., **32**, 3480 (2020).
24. M. Ghidiu, M. R. Lukatskaya, M. Q. Zhao, Y. Gogotsi and M. W. Barsoum, Conductive two-dimensional titanium carbide 'clay' with high volumetric capacitance, *Nature*., **516**, 78 (2014).
25. M. Ghidiu, J. Halim, S. Kota, D. Bish, Y. Gogotsi and M. W. Barsoum, Ion-Exchange and Cation Solvation Reactions in Ti_3C_2 MXene, *Chem. Mater*., **28**, 3507 (2016).
26. H. Pazniak, M. Benchakar and T. Bilyk, Ion Implantation as an Approach for Structural Modifications and Functionalization of Ti_3C_2Tx MXenes. *ACS Nano*.,**15**, 4245 (2021).
27. C. B. Cockreham, X. Zhang, H. Li, E. Hammond-Pereira, J. Sun, S. R. Saunders, Y. Wang, H. Xu and D. Wu, Inhibition of $AlF_3 \cdot 3H_2O$ impurity formation in Ti_3C_2Tx MXene synthesis under a unique CoFx/HCl etching environment, *ACS Appl. Energy Mater*., **2**, 8145 (2019).
28. J. Xuan, Z. Wang, Y. Chen, D. Liang, L. Cheng, X. Yang, Z. Liu, R. Ma, T. Sasaki and F. Geng, Organic-base-driven intercalation and delamination for the production of functionalized titanium carbide nanosheets with superior photothermal therapeutic performance, *Angew. Chem. Int. Ed*., **55**, 14569 (2016).
29. T. Li, L. Yao, Q. Liu, J. Gu, R. Luo, J. Li, X. Yan, W. Wang, P. Liu, B. Chen, W. Zhang, W. Abbas, R. Naz and D. Zhang, Fluorine-free synthesis of high-purity Ti_3C_2Tx (T=OH, O) *via* alkali treatment, *Angew. Chem. Int. Ed*., **57**, 6115 (2018).
30. S. Yang, P. Zhang, F. Wang, A. G. Ricciardulli, M. R. Lohe, P. W. M. Blom and X. Feng, Fluoride-free synthesis of two-dimensional titanium carbide (MXene) using a binary aqueous system, *Chemistry*., **130**, 15717 (2018).
31. W. Sun, S. A. Shah, Y. Chen, Z. Tan, H. Gao, T. Habib, M. Radovic and M. J. Green, Surface-agnostic highly stretchable and bendable conductive MXene multilayers, *Chem. Mater*., **5**, 21663 (2018).
32. Y. Li, H. Shao, Z. Lin, J. Lu, L. Liu, B. Duployer, P. O. Å. Persson, P. Eklund, L. Hultman, M. Li, K. Chen, X.-H. Zha, S. Du, P. Rozier, Z. Chai, E. Raymundo-Piñero, P. L. Taberna, P. Simon and Q. Huang, A general Lewis acidic etching route for preparing MXenes with enhanced electrochemical performance in non-aqueous electrolyte, *Nat. Mater*., **19**, 1 (2019).
33. M. Naguiib, M. Kurtoglu, V. P. Resser, J. Lu, J. J. Niu, M. Heon, L. Hultman, Y. Gogotsi and M. W. Barsoum, A general Lewis acidic etching route for preparing MXenes with enhanced electrochemical performance in non-aqueous electrolyte, *Adv. Mater*., **23**, 4248 (2011).
34. Z. W. Zhang, H. N. Li, D. Guo, J. Hu, B. Z. Liu, Q. R. Zhang and Q. M. Peng, Self-reduction synthesis of new MXene/Ag composites with unexpected electrocatalytic activity, *ACS Sustainable Chem. Eng*., **4**, 6763 (2016).
35. L. Xu, F. Zhao, J. Y. Nong, K. Cheng and Y. Zhang, Preparation, characterization and electro-catalytic properties investigation of lead dioxide electrode, *Tech. Equip. Environ. Pollut. Control*., **07**, 959 (2008).
36. X. M. Cheng, L. H. Zu, Y. Jiang, D. L. Shi, X. M. Cai, Y. H. Ni, S. J. Lin and Y. Qin, A titanium-based photo-Fenton bifunctional catalyst of mp-MXene/TiO_2-x nanodots for dramatic enhancement of catalytic efficiency in advanced oxidation processes, *Chem. Commun*., **54**, 11622 (2018).
37. Z. Othman, A. Sinopoli, H. R. Mackey, K. A. Mahmoud, Efficient Photocatalytic Degradation of Organic Dyes by AgNPs/TiO_2/$Ti_3C_2T_x$ MXene Composites under UV and Solar Light, *ACS Omega*., **6**, 33325 (2021).
38. W. R. Cui, C. Chen, Q. Yu, W. Zhu, H. Wang and H. X. Li, Nano-CeO_2 particles modified titanium-based lead dioxide composite electrode material for oxygen evolution electrocatalytic activity, *Chem. Res. Apply*., **29**, 1380 (2017).
39. M. E. Makgae, C. C. Theron, W. J. Przybylowicz and A. M. Crouch, Preparationand surface characterization of Ti/SnO_2-RuO_2-IrO_2 thin films as electrode material for the oxidationof phenol, *Mater. Chem. Phys*., **92**, 559 (2005).
40. X. Gu, Y. Yang, Y. Hu, M. Hu, J. Huang and C. Wang, Nitrogen-doped graphene composites as efficient electrodes with enhanced capacitive deionization performance, *RSC Adv*., **4**, 63189 (2014).
41. G. Kang, Y. Chen and J. Li, Comparison of structure and electrochemical properties of NiAl, Coal and Nicoal hydroxides, *J. Inorg. Mater.*, **11**, 1230 (2016).
42. Y. Wang, A. G. El-Deen, P. Li, B. H. Oh, Z. Guo, M. M. Khin, Y. S. Vikhe, J. Wang, R. G. Hu and R. M. Boom, High performance capacitive deionization disinfection of water with graphene oxide- graft -quaternized chitosan nanohybrid electrode coating, *ACS Nano*., **9**, 10142 (2015).
43. Z. Zheng, M. S. Thesis, Research on ni-based ceria composite hydrogen evolution reaction

electrode prepared by electrodeposition method, *Harbin Inst. Technol.* (China), (2013).

44. W. D. Li, H. Y. Yang and Q. Liu, Hydrothermal Synthesis of PbO_2/RGO Nanocomposite for Electrocatalytic Degradation of cationic red X-GRL, *J. Nanomater*., **2017**, 1798706 (2017).
45. J. E. L. Santos, D. C. de Moura, D. R. da Silva, M. Panizza and C. A. Martinez-Huitle, Application of TiO_2-nanotubes/PbO_2 as an anode for the electrochemical elimination of Acid Red 1 dye, *J. Solid State Electrochem*., **23**, 351 (2019).
46. D. Chianca De Moura, M. Cerro-Lopez, M. A. Quiroz, D. Ribeiro da Silva and C. A. Martinez-Huitle, Large disk electrodes of Ti/TiO_2-nanotubes/PbO_2 for environmental applications, *RSC Adv*., **5**, 31454 (2015).
47. M. Xu, Y. L. Mao, W. L. Song, X. M. OuYang, Y. H. Hu, Y. J. Wei, C. G. Zhu, W. Y. Fang, B. C. Shao and R. Lu, Preparation and characterization of Fe-Ce co-doped Ti/TiO_2 NTs/PbO_2 nanocomposite electrodes for efficient electrocatalytic degradation of organic pollutants, *J. Electroanal. Chem*., **823**, 193 (2018).
48. K. L. Sun, D. Yuan, Y. Liu, Y. Son, Z. Q. Sun and R. T. Liu, Study on the efficiency and mechanism of Direct Red 80 dye by conventional ozonation and peroxone (O_3/H_2O_2) treatment, *Sep. Sci. Technol*., **55**, 3175 (2020).